Heterogeneity in Serpin−Protease Complexes As Demonstrated by Differences in the Mechanism of Complex Breakdown†

Michael I. Plotnick,*,‡ Madhurika Samakur,‡ Zhi Mei Wang,§ Xhuzuo Liu,§ Harvey Rubin,§ Norman M. Schechter,|| and Trevor Selwood||

Pulmonary, Allergy, and Critical Care Division and Departments of Medicine, Microbiology, and Dermatology, University of Pennsylvania, Philadelphia, Pennsylvania 19104

Received August 7, 2001; Revised Manuscript Received October 29, 2001

ABSTRACT: Serpins trap their target proteases in the form of an acyl-enzyme complex. The trap is kinetic, however, and thus serpin−protease complexes ultimately break down, releasing a cleaved inactive serpin and an active protease. The rates of this deacylation process vary greatly depending on the serpin−protease pair with half-lives ranging from minutes to months. The reasons for the diversity in breakdown rates are not clearly understood. In the current study, pH and solvent isotope effects were utilized to probe the mechanism of breakdown for an extremely stable complex and several unstable complexes. Two different patterns for the pH dependence of k_{bkdn}, the first-order rate constant of breakdown, were found. The stable complex, which breaks down at neutral pH with a half-life of approximately 2 weeks, exhibited a pH−k_{bkdn} profile consistent with solvent−hydroxide ion mediated ester hydrolysis. There was no evidence for the participation of the catalytic machinery in the breakdown of this complex, suggesting extensive distortion of the active site. The unstable complexes, which break down with half-lives ranging from minutes to hours, exhibited a bell-shaped pH profile for k_{bkdn}, typical of the pH−rate profiles of free serine proteases. In the low to neutral pH range k_{bkdn} increased with increasing pH in a manner characteristic of His57-mediated catalysis. In the alkaline pH range a decrease in k_{bkdn} was observed, consistent with the titration of the Ile16-Asp194 salt bridge (chymotrypsinogen numbering). The alkaline pH dependence was not exhibited in pH−rate profiles of free or substrate-bound HNE, indicating that the salt bridge was significantly destabilized in the complexed protease. These results indicate that breakdown is catalytically mediated in the unstable complexes although, most likely, the protease is not in its native conformation and the catalytic machinery functions inefficiently. However, a mechanism in which breakdown is determined by the equilibrium between distorted and undistorted forms of the complexed protease cannot be completely dismissed. Overall, the results of this study suggest that the protease structure in unstable complexes is distorted to a lesser extent than in stable complexes.

Serpins are a superfamily of glycoproteins, the primary physiological role of which is the inhibition of serine proteases. The study of serpin structure and inhibitory mechanism has not only provided significant insights into a number of disease processes but has also forced a reexamination of many notions regarding serine protease inhibition and protein−protein interactions. Instead of the high-affinity, noncovalent binding common to many protease−antiprotease interactions, serpins capture their target proteases as covalent, acyl-enzyme-type complexes, which represent an intermediate of catalysis (*2*−*5*). The current model of the serpin mechanism postulates that cleavage of the reactive site P1−P1′[1] bond of the serpin triggers a large conformational change, which in turn results in the forceful apposition of the protease with the serpin body. Nonspecific steric and charge clashes between surface residues of the serpin and protease lead to a structural rearrangement of the protease and a marked decrease and/or complete abrogation of its catalytic activity (*6*−*14*). The protease therefore remains covalently bound to the P1 residue of the serpin because rapid deacylation cannot be achieved. The recently solved X-ray crystal structure of the complex between α-1-protease inhibitor (PI)[2] and trypsin underscored the extent to which

† This work was supported by funding from the National Institutes of Health grants. HL-03495, HL-50523, AR-42931 and the American Lung Association.

* Correspondence should be addressed to this author. Phone: 215-662-6474; Fax 215-573-2033. E-mail: mplotnic@mail.med.upenn.edu.

‡ Pulmonary, Allergy, and Critical Care Division.

§ Departments of Medicine and Microbiology.

|| Department of Dermatology.

[1] By convention, serpin reactive loop residues are numbered on the basis of the nomenclature of Schechter and Berger (*1*) for substrates and proteases. Serpin P1−P1′ residues are the residues that border the scissile bond. Residues extending toward the N-terminus of the serpin are numbered P1, P2, P3, ..., P*n*, and residues extending toward the C-terminus are numbered P1′, P2′, P3′, ..., P*n*′. The corresponding binding sites on the protease are numbered S*n*, ..., S3, S2, S1, S1′, S2′, ..., S*n*′. The S1 subsite of the protease is the major determinant of specificity.

[2] Abbreviations: ACT, α-1-antichymotrypsin; rACT, recombinant α-1-antichymotrypsin; PI, α-1-protease inhibitor; HNE, human neutrophil elastase; CMK, chloromethyl ketone; SDS−PAGE, sodium dodecyl sulfate−polyacrylamide gel electrophoresis; DTT, dithiothreitol; MeOSucAAPV-NA, *N*-methoxysuccinyl-Ala-Ala-Pro-Val-*p*-nitroaniline; SucAAPV-NA, succinyl-Ala-Ala-Pro-Val-*p*-nitroaniline; SucAAPF-NA, succinyl-Ala-Ala-Pro-Phe-*p*-nitroaniline; TLCK, tosyl-Lys chloromethyl ketone.

10.1021/bi015650+ CCC: $22.00
Published on Web 12/06/2001

the protease structure can be distorted (*12*). The active site structure was grossly altered, and overall approximately 40% of the structure of trypsin was so disordered (or flexible) that it could not be resolved.

Gross changes in the conformation of the protease, such as those demonstrated by the PI−trypsin complex, clearly would be expected to abrogate any catalytic activity of the protease and might even be expected to result in irreversible loss of enzyme activity. However, it has long been appreciated that many serpin−protease complexes spontaneously break down over time, releasing active enzyme and inactive reactive loop cleaved serpin (*15*). The rates of complex breakdown vary enormously, and depending on the serpin−protease complex and buffer conditions half-lives can range from minutes to weeks or even longer (*12*, *16*−*20*). We previously described a series of serpin−human neutrophil elastase (HNE) complexes that demonstrated a broad range of breakdown behaviors. Complexes between recombinant α-1-antichymotrypsin, rACT and its variants, and HNE demonstrated half-lives for complex breakdown that ranged from 30 min to 24 h at pH 8.0, depending on the serpin and salt concentrations. Complexes between HNE and PI formed considerably more "stable" complexes and demonstrated no significant spontaneous complex breakdown after 24 h. While the essentially irreversible inhibition of HNE by PI can be rationalized by a disruption of the catalytic machinery, the considerably more short-lived inhibition of HNE by the rACT variants suggests the possibility of complexes with less extensive distortion of the protease structure and thus residual catalytic activity.

In the experiments described in the current report we determined the effects of pH and D_2O on a series of rACT−HNE complexes in order to investigate the role of the catalytic machinery in the breakdown process. The pH dependence of the PI−HNE complex was evaluated to contrast the behavior of stable and unstable complexes. The effect of salt on complex breakdown was also studied because of earlier observations that breakdown rates for some serpin−HNE complexes increase with increased salt concentrations (*18*, *20*). The results of these studies suggest that the spontaneous breakdown observed for rACT−HNE complexes is due to the inefficient catalytic activity of a distorted although not completely disrupted active site. In contrast, HNE appears to be devoid of catalytic activity when in complex with PI, and breakdown is largely dependent upon a solvent−hydroxide ion mediated process.

EXPERIMENTAL PROCEDURES

Materials. HNE was obtained from Athens Research and Technology (purified from blood neutrophil) and Elastin Products (purified from sputum). TLCK-treated bovine pancreatic α-chymotrypsin (chymotrypsin) was from Worthington. Human plasma PI was from Miles (Prolastin). Substrates and MeOSucAAPV-CMK were from Bachem. *N*-Dodecyl β-D-maltoside (dodecyl maltoside) was from Anatrace. 99.9% D_2O was purchased from Aldrich.

Construction, Expression, and Purification of rACT Variants. The construction of the ACT expression vector pACT, expression, and the purification of recombinant ACT have been described previously (*18*, *21*). Recombinant ACT is expressed in E*scherichia coli* strain N4801 and does not require refolding.

Expression, Refolding, and Purification of rPI. The cDNA for PI was purchased from ATCC and subcloned into the *Nhe*I site of the PET11A expression vector (Novagen). rPI was expressed in *E. coli* strain BL21(DE3) at 37 °C and was induced by the addition of 0.5 mM IPTG. The vast majority of the recombinant protein is found with the cell pellet so rPI was refolded using the Gdn-HCl denaturation and continuous dilution method described by Bottomley and Stone (*22*). Refolded protein was purified on a Fast Q anion-exchange column and eluted with a 50−400 mM NaCl gradient in 10 mM Tris, pH 8.0, buffer. Approximately 1−2 mg of >90% pure rPI (by Coomasie stained gel) was obtained from a 1 L expression.

Determination of Protease Concentrations. Chymotrypsin concentration was determined assuming a specific activity of 3.0 μmol of product (nmol of chymotrypsin)$^{-1}$ min^{-1} measured under standard chymotrypsin assay conditions: 0.4 M Tris, pH 8.0, 1.8 M NaCl, 1 mM SucAAPF-NA (substrate), and 9% DMSO (*23*). This value represents the mean of multiple chymotrypsin solutions which underwent active site titration with *N-trans*-cinnamoylimidazole (*24*). HNE concentrations were determined assuming a specific activity of 0.6 μmol of product (nmol of HNE)$^{-1}$ min^{-1} measured under standard HNE assay conditions: 0.1 M Hepes, pH 7.5, 0.5 M NaCl, 1 mM MeOSucAAPV-NA (substrate), and 9% DMSO. The specific activity was determined by active site titration of HNE with PI (*20*). The concentration of *p*-nitroaniline formed was determined using a molar extinction coefficient at 410 nm of 8800 cm^{-1} M^{-1}.

Determination of Inhibitor Concentrations/Inhibitor Activity. The concentrations of active plasma PI, rPI, and rACT variants in stock solutions were estimated by titration of a solution with a known chymotrypsin concentration, assuming a stoichiometry of inhibition of 1 (*20*). SDS−PAGE analysis of titrations with chymotrypsin indicated that serpins were >90% active since essentially all of the serpin formed the high molecular weight complex at $[E]_0 \cdot [I]_0 > 1$.

SDS−PAGE Analysis of Complex Breakdown. The time course of breakdown of complexes between rACT-P3P3′, a variant of rACT, and HNE was followed by SDS−PAGE as previously described (*20*). Complexes were formed using 2.5 μM HNE and a stoichiometric excess of serpin in 0.05 M Hepes, pH 7.5, 0.4 M NaCl, and 0.01% dodecyl maltoside. The excess serpin was utilized in forming the complex to minimize the generation of cleaved forms of complex. Free HNE is able to cleave the complexed serpin (unpublished data). After a 10 min incubation at room temperature, 0.1 mM MeOSucAAPV-CMK (final) was added to inhibit HNE as it was released from the complex. The CMK stock solution was prepared in 90% DMSO, and the final DMSO in the reaction was 9%. The CMK inhibitor was added to prevent cleavage of the complex by HNE released during breakdown as well as to prevent re-formation of the complex with excess serpin. CMK inhibitor at the concentrations used inhibited HNE at a much greater rate than the serpin. Aliquots were withdrawn at selected times, placed in 600 μL Eppendorf tubes, and immediately frozen with liquid nitrogen and stored at −70 °C until all time points were collected. All of the time points were then processed at the same time by the addition of 5× Laemmli buffer followed by boiling samples for 5 min. Complexes were run on a 10% SDS−PAGE gel

as per Bio-Rad protocol. The Bio-Rad Minigel II apparatus was used.

The first-order rate constant for complex breakdown was determined by densitometric analysis of the uncleaved complex bands after being stained with GelCode Blue (Pierce). Changes in the intensity of HNE bands could not be used for analysis because they were too light to obtain reliable densitometric data. The HNE band is diffuse due to multiple glycosylated forms. The average pixel density of the complex band at each time point was measured using NIH Image 1.6. The average pixel density of a 15 min complex served as the reference corresponding to 100% intact complex. The fractional residual complex was then calculated for each time point relative to the 15 min complex. The first-order rate constant for complex breakdown was then obtained by fitting of the fractional residual complex data to a single exponential equation using nonlinear least squares regression.

Determination of Kinetic Constants k_{cat}/K_m, k_{cat}, and K_m for the Hydrolysis of SucAAPV-NA by HNE. The hydrolysis of the substrate was measured spectrophotometrically by monitoring the release of *p*-nitroaniline at 410 nm at room temperature. Values of k_{cat} and K_m were determined from initial velocity vs $[S]_0$ plots, by nonlinear least squares fit of the data to the Michaelis−Menten rate equation. $[S]_0$ of 10 μM to 4 mM were typically used in this analysis. k_{cat}/K_m values were determined by following progress curves for substrate hydrolysis and fitting the data to a single exponential function to obtain k_{obs}. k_{cat}/K_m was then calculated from $k_{obs}/[E]_0$. $[S]_0$ of 5 μM to 40 μM concentrations, 10−20-fold lower than K_m, were typically employed in this analysis.

Determination of the Rate Constant for Complex Breakdown, k_{bkdn}. The breakdown of the serpin−protease complex was measured by monitoring the return of HNE hydrolytic activity over time. Hydrolysis of SucAAPV-NA was measured spectrophotometrically as described above. In a typical experiment, the preformed serpin−HNE complex was diluted approximately 100-fold into the assay buffer: 0.05 M buffer, 0.4 M NaCl (or 2 M NaCl), 1.0 mM substrate, 9% DMSO, and 0.01% dodecyl maltoside. Experiments were performed in 0.4 M NaCl or higher since initial experiments in 0.1 M salt suggested loss of HNE with time. Furthermore, the ionic strength of the various pH buffers varied by less than 10% when higher NaCl concentrations were used.

Progress curves were obtained by measuring absorbance at 410 nm at specific time intervals which ranged from 10 to 60 s for 60−120 min total time. Progress curve data were differentiated using IGOR data analysis software. The first-order rate constant for complex breakdown, k_{bkdn}, was then determined using a nonlinear least squares fit of the velocity (V) vs time plots to the exponential equation:

$$V(t) = (V_c - V_i)e^{-k_{bkdn}t} \quad (1)$$

where V_c is rate of substrate hydrolysis by HNE in the absence of inhibitor determined in a control experiment and V_i is the initial hydrolytic rate of the serpin−HNE reaction mixture; i.e., the residual HNE.

Formation of Serpin−Protease Complexes. Complexes were preformed prior to dilution in the appropriate buffer for the measurement of breakdown rates. Titrations of HNE with each serpin were performed as previously described (*20*) in order to determine the volume of serpin stock solution required to fully inhibit HNE in the complex-forming reaction. Complexes were then prepared using sufficient serpin to inhibit HNE activity approximately 95%. Initial concentrations of 1.0−1.2 μM HNE were used. Complexes were prepared in 0.1 M MOPS or Hepes, pH 7.5, 0.4 M NaCl, and 0.01% dodecyl maltoside buffer. Typically, enough complex was prepared for four breakdown assays to be performed concurrently.

Table 1: Reactive Loop Sequences for ACT, rACT Variants, and PI

Inhibitor	Reactive loop
	358
	P15 P6 P1 P1' P5'
ACT	GTEASAATAVKITL**L**SALVE
rACT-L358M	**M**
rACT-P3P3'	IP**M**SIP
rACT-P4P3'	AIP**M**SIP
PI	GTEAAGAMFLEAIP**M**SIPPE

Determination of pK_a Values. pK_a values were determined for k_{cat} and k_{cat}/K_m for the hydrolysis of SucAAPV-NA by HNE as well as for k_{bkdn} of serpin−HNE complexes. pH−rate data were evaluated using nonlinear least squares fits of the data to eq 2 or 3 below (*23*). Logarithmic transformed data were used in the fits as recommended by Cleland (*25*). Equation 2 was used when pH−rate profiles appeared to be consistent with a model in which deprotonation of a single ionizable group controlled enzyme activity. Equation 3 was used for bell-shaped profiles, consistent with a model in which there are two ionizable groups on the enzyme but only one active form. k_{pH} is the pH-sensitive rate constant being measured, and k_{lim} is the magnitude of this rate constant if 100% of the enzyme were in the active ionized form. Buffers

$$\log k_{pH} = \log\left(\frac{k_{lim}}{1 + 10^{pK_1 - pH}}\right) \quad (2)$$

$$\log k_{pH} = \log\left(\frac{k_{lim}}{1 + 10^{pK_1 - pH} + 10^{pH - pK_2}}\right) \quad (3)$$

used for the various pHs were as follows: Mes (5.5−6.0), MOPS (6.5−7.0), Hepes (7.0−7.5), Tris (8.0−8.5), CHES (9.0−9.5), and CAPS (10.0−11).

Solvent Isotope Effects. These experiments were performed using essentially the same methodology as the experiments in water. pD was measured using the empiric relation: pD = meter reading + 0.4 (*26*). Assay buffer solutions utilized the same set of buffers as described for the various pH ranges. The final atom fraction of deuterium was ≥0.9. Complexes were produced in water and diluted 50−100-fold into assay buffer.

Data Analysis. The program Igor from Wavemetrics was used for the above analyses.

RESULTS

Serpin−HNE Complexes. The serpins utilized in this study and the reactive loop sequences are shown in Table 1. The

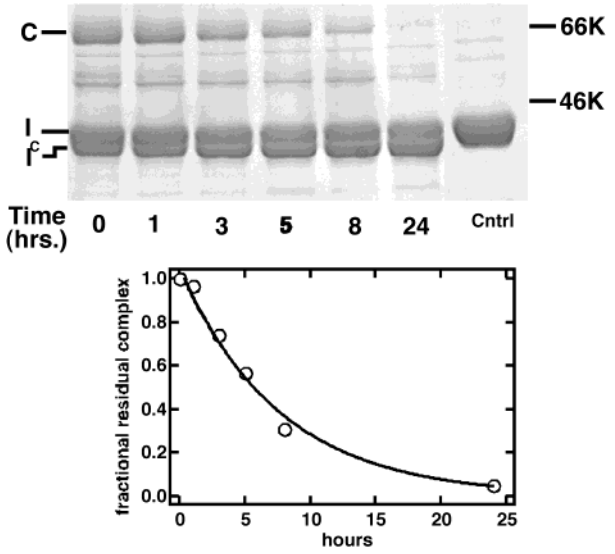

FIGURE 1: SDS−PAGE analysis of rACT-P3P3′−HNE breakdown. Top panel: SDS−PAGE of the time course for the breakdown of rACT-P3P3′−HNE complex in 0.05 M Hepes, pH 7.5, 0.4 M NaCl, and 0.01% dodecyl maltoside buffer. Bands are labeled as follows: C, complex; I, native inhibitor; I^c, reactive loop cleaved inhibitor. An excess of inhibitor was used to form the complex to minimize degradation of the complex by HNE (the serpin component of the complex is degraded). The cleaved inhibitor observed in the first lane is a consequence of the stoichiometry of inhibition of 1.4 for this reaction. MeOSucAAPV-CMK was used to inhibit HNE released from the complex and prevent formation of a new complex. The HNE band on SDS−PAGE is diffuse and difficult to resolve because of a variable extent of glycosylation. It is not shown in this figure. Bottom panel: Plot of the fractional residual complex vs time. The fractional residual complex was determined by densitometry as described in Experimental Procedures. The solid line represents a fit of the data to a single exponential.

three recombinant ACT variants are all ACT−PI chimeras in which one to seven residues in the region of the P1 site of ACT was replaced by the corresponding residues from PI. The inhibitory characteristics with HNE, (i) second-order inhibition rate constant, (ii) stoichiometry of inhibition, and (iii) breakdown rates at pH 8.0, 0.1 M NaCl buffer, have been described previously (*20*).

SDS−PAGE Analysis of Breakdown of rACT-P3P3′−HNE Complexes. SDS−PAGE analysis of the breakdown of rACT-P3P3′−HNE complex was performed in order to determine the relationship between the return of HNE activity and hydrolysis of the covalent bond between the serpin and protease. Hydrolysis of the acyl-enzyme may not be the rate-determining step in the return of HNE activity if tight noncovalent interactions exist between the serpin and protease and/or if the protease regains activity slowly following complex breakdown. A gel of the rACT-P3P3−HNE complex time course is shown at the top of Figure 1. At the bottom of Figure 1 is a plot of the densitometric data fit to a simple exponential curve. The first-order rate constant of complex breakdown, k_{bkdn}, determined from the disappearance of complex was $(2.3 \pm 0.2) \times 10^{-3}$ min^{-1}, which is the essentially the same rate constant obtained by following return of HNE activity (*20*). Thus, the return of HNE activity parallels hydrolysis of the covalent serpin−protease bond.

pH Profile for Complex Breakdown of rACT−HNE Complexes. pH−breakdown rate profiles were obtained for three rACT−HNE complexes, all of which demonstrate spontaneous breakdown, to examine the mechanism(s)

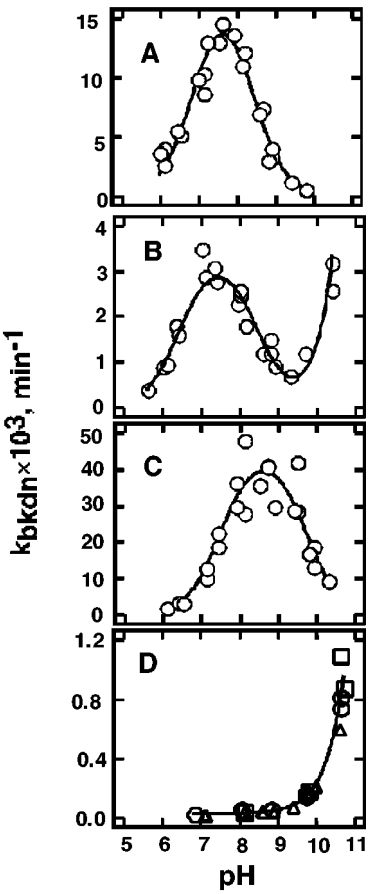

FIGURE 2: pH−k_{bkdn} profiles for the breakdown of rACT−HNE complexes in 0.4 M NaCl and PI−HNE complexes at 0.4 and 2 M NaCl. k_{bkdn} were measured as described in Experimental Procedures. Panels A−C represent data obtained on the breakdown of preformed rACT−HNE complexes in 50 mM buffer containing 0.4 M NaCl and 0.01% dodecyl maltoside. Panels: A, rACT-L358M−HNE; B, rACT-P3P3′−HNE; C, rACT-P4P3′−HNE. Each open circle corresponds to a single data point. Solid lines represent curves generated with parameters obtained from nonlinear fits to eq 3 (panels A and C) and eq 4 (panel B) as described in Experimental Procedures and Results. Log k_{bkdn} vs pH data were actually used for the fits. Panel D: PI−HNE complexes with plasma-purified PI in 0.4 M NaCl, open circles; PI in 2 M NaCl, open triangles; and rPI in 2 M salt, open squares. The solid line was generated using fit parameters from eq 5 as described in Results.

for cleavage of the acyl-enzyme. NaCl concentrations of 0.4 M were used because loss of HNE activity in control experiments was observed with lower concentrations of salt.

The results of pH−breakdown rate studies for the three rACT−HNE complexes are shown in Figure 2, panels A−C. A bell-shaped profile was observed for rACT-P4P3′−HNE and rACT-L358M−HNE complexes. Log transformed pH−k_{bkdn} data for these complexes were well fit by eq 3 (see Experimental Procedures) and provided values for k_{lim}, pK_a1, and pK_a2. The pattern exhibited by the rACT-P3P3′−HNE complex was more complicated: a bell-shaped relationship followed by a second increase in k_{bkdn} that becomes apparent at approximately pH 10. This third process was postulated to represent the contribution of hydroxyl ion mediated breakdown that was apparent on the rACT-P3P3′−HNE profiles because of the significantly lower k_{bkdn} rates. Thus, eq 3 was altered to take into account the contribution of hydroxide ion mediated deacylation. The log transformed

Table 2: Fit Parameters for k_{lim}, pK_a1, and pK_a2

serpin	$k_{lim} \times 10^3$ (min^{-1})	pK_a1	pK_a2
	0.4 M NaCl		
rACT-L358M	17 ± 2	6.7 ± 0.1	8.3 ± 0.1
rACT-P3P3′[a]	3.4 ± 0.3	6.4 ± 0.1	8.4 ± 0.1
rACT-P4P3′	46 ± 4	7.55 ± 0.1	9.7 ± 0.1
	2.0 M NaCl		
rACT-L358M	40 ± 6	6.9 ± 0.15	8.6 ± 0.1
rACT-P3P3′	23 ± 4	7.3 ± 0.1	8.5 ± 0.1
rACT-P4P3′	37 ± 4	7.3 ± 0.1	10.1 ± 0.1

[a] $k_{OH^-} = 13 \pm 2$ M^{-1} min^{-1} was also obtained from the fit of the rACT-P3P3′−HNE complex to eq 4.

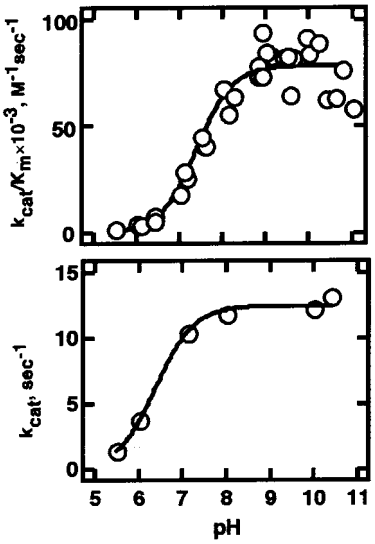

FIGURE 3: pH−rate profiles for HNE hydrolysis of SucAAPV-NA in 0.4 M NaCl containing buffer. Top panel: k_{cat}/K_m. Bottom panel: k_{cat}. Solid lines represent curves generated using parameters from a fit of the data to eq 2.

pH−rate profile for the rACT-P3P3′−HNE complex was well fit by the equation:

$$\log k_{pH} = \log\left(\frac{k_{lim}}{1 + 10^{pH-pK_1} + 10^{pH-pK_2}} + k_{OH^-} \times 10^{pH-pK_w}\right) \quad (4)$$

k_{OH^-} represents the second-order rate constant for hydroxide ion mediated complex breakdown.

The results of the fit parameters k_{lim}, pK_{a1}, and pK_{a2} are shown in Table 2. k_{lim} was slowest for rACT-P3P3′−HNE and fastest for rACT-P4P3′−HNE complexes, with at least an order of magnitude difference between the two. The same relationship in complex breakdown rates between the three chimeras was observed using k_{bkdn} values at pH 8.0 and 0.1 M NaCl determined without dilution of the complex and utilizing a discontinuous assay method (*20*).

The pK_a1 values ranged from 6.4 to 7.55 (Table 2) for the three complexes. These values are consistent with the ionization constant attributed to His57 of the active site of chymotrypsin−trypsin family proteases. The increase in k_{bkdn} (see Figure 2A−C) as pH is increased from the acidic to slightly alkaline range is also characteristic of serine protease activity and reflects the function of His57 as a general base catalyst. In Figure 3 the pH−rate profiles for the hydrolysis of the model substrate SucAAPV-NA by HNE are demonstrated. pK_as of 7.4 and 6.2 were obtained from the analysis under k_{cat}/K_m and k_{cat} conditions, respectively. Stein et al. (*27*) have reported similar pK_as of 7.2 and 6.1 for the k_{cat}/K_m and k_{cat} for the hydrolysis of the closely related substrate MeOSucAAPV-NA by HNE.

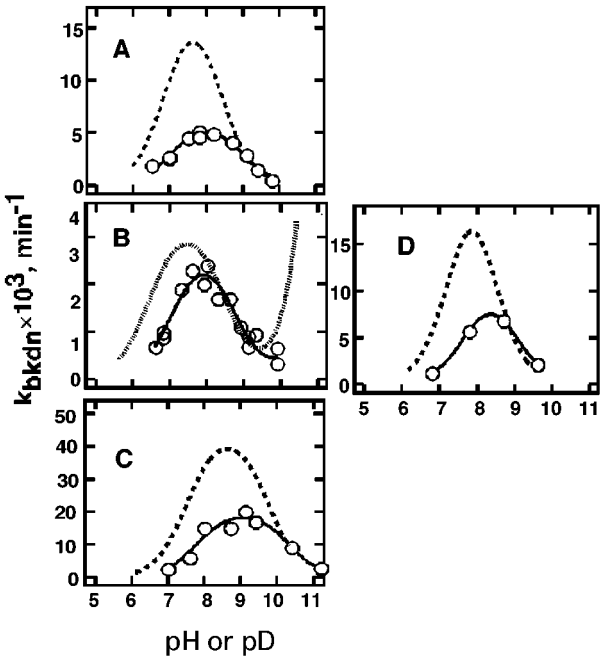

FIGURE 4: pH− or pD−k_{bkdn} profiles for the breakdown of serpin−protease complexes in D_2O buffers. Panels: A, rACT-L358M−HNE in 0.4 M NaCl; B, rACT-P3P3′−HNE in 0.4 M NaCl; C, rACT-P4P3′−HNE in 0.4 M NaCl; D, rACT-P3P3′−HNE in 2 M NaCl. The solid lines represent curves generated from fits of the data to eqs 3 and 4 as described in Results. The hatched lines represent the fits of the corresponding complexes in H_2O.

The apparent pK_a values for the high-pH process, pK_a2, were 9.7 for rACT-P4P3′−HNE, 8.3 for rACT-L358M−HNE, and 8.4 for rACT-P3P3′−HNE. A bell-shaped curve was not observed in pH−rate profiles for the hydrolysis of SucAAPV-NA or MeOSucAAPV-NA (*27*) by HNE but is exhibited by chymotrypsin A, in which pK_a2 for α-chymotrypsin is 8.8 and for δ-chymotrypsin is 9.1 (*28*). The high-pH effect has been shown to correspond to the titration of the α-amino group of Ile16 which forms a salt bridge with Asp194, a critical structure in all serine proteases of the chymotrypsin−trypsin family.

Solvent−Isotope Effects on the Kinetics of Complex Breakdown. Solvent isotope effects on breakdown rates of serpin complexes were studied to further characterize the rate-determining step(s) of complex breakdown. The effects of D_2O on the hydrolysis of substrates by serine proteases, including HNE, have been extensively studied (*27*, *29*, *30*). A 2−4-fold decrease in k_{bkdn} is expected if His57-mediated general base catalysis is the rate-limiting step. Plots of k_{bkdn} versus pD are shown in Figure 4. The complexes continued to demonstrate a bell-shaped relationship and, as expected, are shifted rightward toward a higher pD. The kinetic parameters k_{lim}, pK_a1, and pK_a2 were determined by fitting log transformed data for rACT-P4P3′−HNE and rACT-L358M−HNE complexes to eq 3. The rACT-P3P3′−HNE complex was again fit to eq 4 (using the pK_w for D_2O). The k_{lim}, pK_a1, pK_a2, and $k_{lim,H_2O}/k_{lim,D_2O}$ are shown in Table 3.

Table 3: Solvent Isotope Effects on k_{bkdn}

serpin	[NaCl] (M)	$k_{lim} \times 10^3$ (min^{-1})	pK_a1	pK_a2	k_{H_2O}/k_{D_2O}
rACT-Met	0.4	6.1 ± 0.1	7.0 ± 0.1	8.9 ± 0.1	2.8 ± 0.1
rACT-P3P3′	0.4	2.8 ± 0.5	7.1 ± 0.15	8.7 ± 0.15	1.4 ± 0.2
	2.0	11.0 ± 1.0	7.7 ± 0.2	9.0 ± 0.2	2.0 ± 0.2
rACT-P4P3′	0.4	20.0 ± 2.0	7.85 ± 0.1	10.4 ± 0.1	2.3 ± 0.1

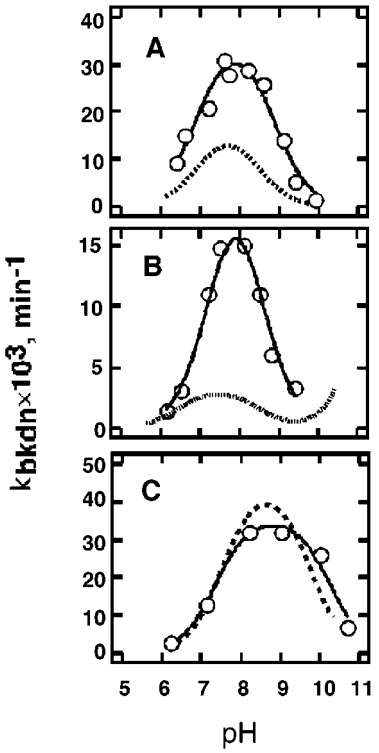

FIGURE 5: pH−k_{bkdn} profiles for the breakdown of rACT−HNE complexes in 2 M salt. Panels: A, rACT-L358M−HNE; B, rACT-P3P3′−HNE; C, rACT-P4P3′−HNE. The hatched lines are the same curves shown in Figure 1 for the corresponding complexes.

Solvent isotope effects of >2 were observed for the rACT-P4P3′−HNE and rACT-L358M−HNE complexes, but the solvent isotope effect was 1.4 for rACT-P3P3′−HNE in 0.4 M NaCl buffer. The smaller solvent isotope effect suggests that His57-mediated hydrolysis is partially rate determining for this complex. Alternatively, $k_{lim,H_2O}/k_{lim,D_2O}$ might be underestimated due to effects of the D_2O on solvent or protein structure.

Effects of High Salt on the pH−Rate Profiles of Complex Breakdown. pH−rate profiles for the rACT−HNE complexes with HNE were determined in 2 M NaCl in order to further characterize the NaCl-induced acceleration of breakdown previously described for the rACT-P3P3′−HNE and rACT-L358M−HNE complexes (*18*, *20*). All three complexes again demonstrated bell-shaped profiles as shown in Figure 5. k_{lim}, pK_a1, and pK_a2 values are shown in the bottom of Table 2. High salt concentrations increased k_{lim} almost 7-fold for rACT-P3P3′−HNE complexes. The effect of salt on rACT-P3P3′−HNE complexes was reversible since production of the complex at pH 8 and 2 M salt did not significantly change k_{bkdn} determined in 0.4 M salt buffer. A 2-fold increase was noted for rACT-L358M−HNE, while the magnitude of k_{lim} for the rACT-P4P3′−HNE complex was essentially unchanged. Overall, k_{lim} values are remarkably similar for all three rACT−HNE complexes in high salt.

The effects of high salt on pK_a1 were variable. pK_a1 for rACT-P3P3′−HNE increased from 6.4 to 7.3. In contrast, the pK_a1 for rACT-L358M−HNE and rACT-P4P3′−HNE did not change significantly. Minimal change was also observed in pK_a2 for the three complexes between 0.4 and 2.0 M salt. The difference of 1.5 pK_a units between rACT-P4P3′−HNE and the other two complexes persisted.

High salt also affected $k_{lim,H_2O}/k_{lim,D_2O}$ for rACT-P3P3′−HNE, increasing the solvent isotope effect to 2.0 (see Figure 4D and Table 3). His57-mediated catalysis therefore appears to be the predominant rate-limiting step for breakdown of this complex under high salt concentrations.

Studies on SucAAPV-NA hydrolysis by HNE in buffer containing 2 M NaCl (data not shown) demonstrated essentially the same pK_a profiles for k_{cat} and k_{cat}/K_m as in 0.4 M NaCl containing buffer. K_m values were lower in 2 M NaCl buffer.

pH Effect on the Breakdown of PI−HNE Complexes. The pH−breakdown rate profiles were determined for PI−HNE complexes in order to compare the breakdown process of the relatively unstable complex with a complex that we previously found did not demonstrate appreciable return of HNE activity after 24 h in 0.8 M NaCl. However, all of the HNE activity was recovered by treating the PI−HNE complexes with hydroxylamine. HNE activity returned with a half-life of approximately 5 h and is essentially complete 24 h after the addition of 1 M hydroxylamine at pH 8.0 (data not shown). The ability to recover 100% of active HNE indicates that HNE is not irreversibly modified in the complex with PI.

The breakdown assay used in the current study for PI−HNE complexes was designed to detect breakdown of <1% of the complex. The pH−k_{bkdn} plot for the PI−HNE complex is shown in Figure 2, panel D. A significantly different relationship was observed from the bell-shaped curves. Breakdown rates for the PI−HNE complex were flat in the neutral pH range and then increased rapidly with increasing pH. No evidence of a plateau at high pH was observed. The breakdown rate constants were considerably smaller than those for the rACT−HNE complexes; only at approximately pH 10.5 do breakdown rates approach that of the rACT-P3P3′−HNE complex in low salt. Similar behavior was demonstrated by recombinant and plasma-derived PI in both 0.4 and 2 M salt conditions. This behavior was suggestive of a hydroxide ion dependent mechanism, and a log k_{bkdn} vs pH plot was well fit by the relationship described in the equation:

$$\log k_{bkdn} = \log(k_{HOH} + k_{OH^-} \times 10^{pH-pK_w}) \qquad (5)$$

k_{HOH} is the pseudo-first-order rate constant of complex breakdown by water and k_{OH^-} is the second-order rate constant for hydroxide ion mediated complex breakdown.

Values for k_{HOH} and k_{OH^-} of $(2.9 \pm 0.4) \times 10^{-5}$ min^{-1} and 0.92 ± 0.01 M^{-1} min^{-1} were obtained.

DISCUSSION

The serpin mechanism of inhibition may be best described as a kinetic trap (*15*). The serpin−protease interaction initially results in the formation of an acyl-enzyme-type complex, but ultimately, hydrolysis of the reactive site bond is completed and an active protease molecule is released.

Breakdown of the covalent complex therefore is analogous to the deacylation step of a substrate reaction but occurs at markedly diminished rates. Complexes that break down with half-lives that exceed weeks have been reported. PI−HNE appears to be such a complex. However, complexes that are considerably shorter lived, with half-lives of minutes to hours, have been described as well. Rapid breakdown rates have generally been observed for complexes formed by wild-type serpins and proteases that are not their true physiological target, such as ACT and chymotrypsin, or for some complexes formed by recombinant serpin variants (*17*, *18*, *20*, *31*). The complexes formed by the rACT variants with HNE represent the more unstable type of complex. These serpins were originally produced in an attempt to convert ACT from a substrate to an inhibitor of HNE (*18*, *20*) using the reactive loop sequence of PI. None of the rACT−HNE complexes demonstrated the extreme stability of the PI−HNE complex, although all were SDS stable, indicating that the return of HNE activity represented the breakdown of an acyl-enzyme complex. In the current study we have investigated pH and solvent effects on the breakdown of rACT−HNE and PI−HNE complexes in order to better understand the mechanism of complex breakdown and the reasons for the apparent divergent behavior of the stable and unstable complexes.

The breakdown of the PI−HNE complex demonstrated a pH dependence consistent with solvent-mediated ester hydrolysis. The half-life of the PI−HNE complex breakdown was approximately 16 days in the neutral pH range, a rate that is approximately 6−8 orders of magnitude slower than the deacylation rates of model peptide substrates by HNE (*32*, *33*). In the high-pH range k_{bkdn} increased in a manner consistent with alkaline-catalyzed hydrolysis. Calugaru et al. (*34*) recently reported a similar pH dependence for a number of long-lived serpin−trypsin complexes, including the PI−trypsin complex. A complete lack of catalytic activity in the serpin-bound protease is not unexpected, considering the degree of conformational rearrangement of the active site observed for trypsin in the X-ray crystal structure of PI−trypsin (*12*). In this complex the reactive loop is fully inserted, and the P1−Met residue has been pulled away from the active site of the protease. As a result, the covalently linked Ser195 of trypsin is displaced 3.5 Å from its position near His57, and the conformation of the peptide backbone of adjacent residues is altered, leading to the disruption of the salt bridge, oxyanion hole, and S1 pocket.

In contrast to the pH dependence of the PI−HNE complex, the three unstable complexes exhibited a bell-shaped pH−rate profile more typical of serine protease activity. The increase in k_{bkdn} over the low to neutral pH range is characteristic of the titration of His57 and indicates that breakdown is catalytically mediated in these complexes. Solvent isotope effects observed for the unstable complexes provide further evidence for His57-mediated general base catalysis (*26*). In the alkaline pH range a decrease in k_{bkdn} was observed with increasing pH. This high pH dependence is a second classical feature of the pH−rate profiles of serine proteases that has been attributed to the titration of a basic structural element, the Ile16-Asp194 salt bridge (*35*−*37*). pK_a2 is an apparent pK_a determined both by the ionization constant of the free α-amino group (7.9 in the case of isoleucine) and by the conformational equilibrium between

Scheme 1

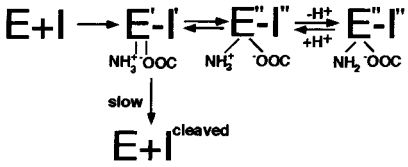

active (salt bridge formed) and inactive (salt bridge dissociated) forms of the protease (*28*, *38*). The apparent absence of the high-pH effect in the pH−rate profiles of free and substrate-bound HNE is therefore an indication of a considerable degree of conformational stability. Conversely, the presence of the high-pH dependence in the breakdown of the unstable complexes is an indication of a marked decrease in the conformational stability of HNE when complexed with the rACT variants. Since pK_a2 of free HNE must significantly exceed pH 11, this apparent ionization constant has been shifted at least 2−3 pH units for the various complexes.

An alternative interpretation of the high-pH effect on rACT−HNE complex breakdown is that Ile16-Asp194 is already disrupted, and titration of a group other than Ile16 is responsible for the apparent loss of catalytic activity in the complexed protease. However, no clear alternative candidate is easily identified. There are no lysine or unpaired cysteines in HNE. Two tyrosine residues are present although they are not in the active site region.

While the presence of the alkaline pH effect on k_{bkdn} suggests a significant destabilization of the Ile16-Asp194 salt bridge, the fact that pK_a2 values for the rACT−HNE complexes remain greater than 7.9 indicates that the salt bridge is formed in a majority of complexes at neutral pH. The overall structural implications of the pH dependence of k_{bkdn} exhibited by the unstable complexes is that HNE maintains a significant degree of native character in the low to neutral pH range although it is not structurally equivalent to the native enzyme. Thus, the structure of HNE in the unstable complexes is not nearly as distorted as the trypsin−PI complex; however, the fundamental mechanism underlying the distortion of the active site is likely the same. That is, strain is applied to Ser195 through the covalently linked P1 residue. Even relatively limited displacement of Ser195 would be expected to decrease the efficiency of His57-mediated catalysis, alter the structure of the oxyanion hole which is composed of the peptide backbones of Ser195 and Gly193, and alter the geometry of the Ile16-Asp194 salt bridge. The positioning of the P1 residue within the active site would also be affected. Deprotonation of Ile16 by high pH would be expected to drive the protease to adopt more distorted structures with a dissociated salt bridge. Whether the high-pH conformation involves global distortion of HNE similar to trypsin in complex with PI or more limited changes is not clear.

The above interpretation of the alkaline pH dependence of k_{bkdn} for the unstable ACT−HNE complexes suggests a mechanism such as that shown in Scheme 1. This minimal scheme focuses on the covalent complex in the alkaline pH range. Complex formation is represented as a simplified single irreversible step. E′−I′ represents a complex form in which the salt bridge is present but the active site geometry is distorted sufficiently to impair catalytic activity. E″−I″

Scheme 2

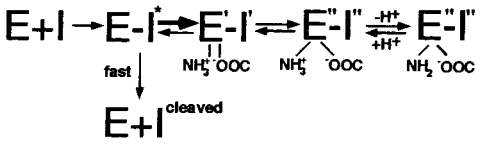

represents forms in which the salt bridge is dissociated and catalytic activity is completely abrogated. $I^{cleaved}$ is the reactive loop cleaved form of the inhibitor that is released upon complex breakdown. In such a mechanism, breakdown rates are 3−5 orders of magnitude less than substrate deacylation rates because the catalytic machinery operates inefficiently. Furthermore, variations in k_{bkdn} between the rACT−HNE complexes represent differences in the residual catalytic activity of the complexed protease as well as differences in the equilibrium between partially active and completely inactive conformations.

An alternative mechanism, in which E′−I′ is devoid of catalytic activity, is shown in Scheme 2. Breakdown rates in this mechanism are determined by a complex form, E−I*, in which HNE retains essentially a native conformation and normal catalytic activity. Although breakdown of the E−I* complex is rapid, overall breakdown is slow because E−I* constitutes only a minute fraction of the total complex. In both Schemes 1 and 2, E′−I′ is a major form when pH is less than pK_a2, and high pH drives the equilibrium toward forms with a dissociated salt bridge. The results of the current study do not unambiguously differentiate between the two schemes. It should be noted that the various conformations of HNE in complex are most likely associated with differences in the extent of insertion of the reactive loop and/or positioning of the protease against the serpin body. The precise structural basis for how differences in reactive loop sequence between the three rACT variants lead to differences in complex stability remains unclear.

The effect of 2 M NaCl on the pH dependence of rACT−HNE complex breakdown was investigated because of an earlier observation that increasing salt concentrations accelerated k_{bkdn} for some of these complexes. Increased breakdown rates and decreased proteolytic sensitivity in high salt have been observed for ACT−chymotrypsin complexes as well (*7*, *17*). These findings suggested that the presence of high salt decreases the extent of distortion of the protease. High salt concentrations favor more compact protein structures (*39*) and could decrease the effect of repulsive charge−charge interactions between the serpin and protease bodies that tend to destabilize the protease structure. However, the results of pH−k_{bkn} studies in 2 M NaCl did not provide clear evidence for a stabilizing effect of high salt on the structure of complexed HNE. pK_a2 increased only minimally for all of the rACT−HNE complexes and did not correlate with changes in k_{lim}. The changes in k_{lim}, pK_a1, and the solvent isotope effect observed for the rACT-P3P3′−HNE complex suggested that HNE may be adopting a less distorted conformation in high salt; however, it is impossible to attribute the changes in these parameters to any particular structural features. The PI−HNE complex did not exhibit any significant effect of high salt on breakdown. In contrast, Calugaru and co-workers (*34*) demonstrated a dramatic effect of calcium on the conformation of trypsin in complex. High concentrations of calcium (10−100 mM) converted the serpin−trypsin complexes mentioned previously in the Discussion from stable to unstable type complexes that exhibited breakdown rates similar to those of the rACT−HNE complexes. Native trypsin contains a high-affinity binding site for calcium (10−100 μM). Thus, the high concentrations of calcium employed in this study provide a substantial thermodynamic driving force for the active conformation.

In conclusion, the relatively rapid breakdown of some serpin−protease complexes appears to result from the inability of the serpin to sufficiently distort the target protease, thereby leaving residual catalytic activity. However, the rACT variants are not defective serpins. On the contrary, these serpins form complexes with human mast cell chymase that are at least as stable as the PI−HNE complex (*20*). Thus, the formation of a stable complex and the maximal distortion of the active site of the complexed protease require more than a nominally functional serpin and translocation of the protease to the bottom of the serpin. The specific structural differences between PI, the physiological inhibitor of HNE, and ACT that allow the former to be so much more effective at distorting the structure of HNE are unclear. Elements in the region of contact between the serpin and protease and/or elements involved in maintaining full insertion of the reactive loop are almost certainly involved. Thus, serpins appear to have evolved not only to rapidly inhibit their physiological target proteases but also to form complexes that can be cleared from tissues or plasma (*40*) and degraded long before any significant breakdown occurs.

REFERENCES

1. Schechter, I., and Berger, A. (1967) *Biochem. Biophys. Res. Commun. 27*, 157−162.
2. Fa, M., Karolin, J., Aleshkov, S., Strandberg, L., Johansson, L. B.-Å., and Nor, T. (1995) *Biochemistry 34*, 13833−13840.
3. Lawrence, D. A., Ginsburg, D., Day, D. E., Berkenpas, M. B., Verhamme, I. M., Kvassman, J.-O., and Shore, J. D. (1995) *J. Biol. Chem. 270*, 25309−25312.
4. Wilczynska, M., Fa, M., Ohlsson, P.-I., and Ny, T. (1995) *J. Biol. Chem. 270*, 29652−29655.
5. Egelund, R., Rodenburg, K. W., Andreasen, P. A., Rasmussen, M. S., Guldberg, R. E., and Petersen, T. E. (1998) *Biochemistry 37*, 6375−6379.
6. Hervé, M., and Ghélis, C. (1991) *Arch. Biochem. Biophys. 285*, 142−146.
7. Stavridi, E. S., O'Malley, K., Lukacs, C. M., Moore, W. T., Lambris, J. D., Christianson, D. W., Rubin, H., and Cooperman, B. S. (1996) *Biochemistry 35*, 10608−10615.
8. Kaslik, G., Patthy, A., Bálint, M., and Gráf, L. (1995) *FEBS Lett. 370*, 179−183.
9. Plotnick, M. I., Mayne, L., Schechter, N. M., and Rubin, H. (1996) *Biochemistry 35*, 7586−7590.
10. Kaslik, G., Kardos, J., Szabó, E., Szilágyi, L., Závodsky, P., Westler, W. M., Markley, J. L., and Gráf, L. (1997) *Biochemistry 36*, 5455−5464.
11. Kaslik, G., Westler, W. M., Graf, L., and Markley, J. (1999) *Arch. Biochem. Biophys. 362*, 254−264.
12. Huntington, J. A., Read, R. J., and Carrell, R. W. (2000) *Nature 407*, 923−926.
13. Egelund, R., Petersen, T. E., and Andreasen, P. A. (2001) *Eur. J. Biochem. 268*, 673−685.
14. Peterson, F. C., and Gettins, P. G. (2001) *Biochemistry 40*, 6284−6292.
15. Gettins, P. G. W., Patston, P. A., and Olson, S. T. (1996) *Serpins: Structure, Function and Biology*, R. G. Landes Co., Austin, TX.

16. Oda, K., Laskowski, M., Kress, L. F., and Kowalski, D. (1977) *Biochem. Biophys. Res. Commun. 76*, 1062−1071.
17. Cooperman, B. S., Stavridi, E., Nickbarg, E., Rescorla, E., Schechter, N., and Rubin, H. (1993) *J. Biol. Chem. 268*, 23616−23625.
18. Rubin, H., Plotnick, M., Wang, Z. M., Liu, X., Zhong, Q., Schechter, N. N., and Cooperman, B. S. (1994) *Biochemistry 33*, 7627−7633.
19. Olson, S. T., Bock, P. E., Kvassman, J., Shore, J. D., Lawrence, D. A., Ginsburg, D., and Björk, I. (1995) *J. Biol. Chem. 270*, 30007−30017.
20. Plotnick, M., Schechter, N. M., Wang, Z. M., Liu, X., and Rubin, H. (1997) *Biochemistry 36*, 14601−14608.
21. Rubin, H., Wang, Z. M., Nickbarg, E. B., McLarney, S., Naidoo, N., Schoenberger, O. L., Johnson, J. L., and Cooperman, B. S. (1990) *J. Biol. Chem. 265*, 1199−1207.
22. Bottomley, S. P., and Stone, S. R. (1998) *Protein Eng. 11*, 1243−1247.
23. Schechter, N. M., Plotnick, M., Selwood, T., WAlter, M., and Rubin, H. (1997) *J. Biol. Chem. 272*, 24499−24507.
24. Schonbaum, G. R., Zerner, B., and Bender, M. L. (1961) *J. Biol. Chem. 236*, 2930−2935.
25. Cleland, W. W. (1979) *Methods Enzymol. 63*, 103−138.
26. Schowen, K. B., and Schowen, R. L. (1982) *Methods Enzymol. 87*, 551−606.
27. Stein, R. (1983) *J. Am. Chem. Soc. 105*, 5110−5116.
28. Fersht, A. R. (1972) *J. Mol. Biol. 64*, 497−509.
29. Stein, R. L., Strimpler, A. M., Hori, H., and Powers, J. C. (1987) *Biochemistry 26*, 1305−1314.
30. Stein, R. L., Strimpler, A. M., Hori, H., and Powers, J. C. (1987) *Biochemistry 26*, 1301−1305.
31. Chaillan-Huntington, C. E., Gettins, P. G. W., Huntington, J. A., and Patston, P. A. (1997) *Biochemistry 36*, 9562−9570.
32. Harper, J. W., Cook, R. R., Roberts, C. J., McLaughlin, B. J., and Powers, J. C. (1984) *Biochemistry 23*, 2995−3002.
33. Stein, R. L. (1985) *Arch. Biochem. Biophys. 236*, 677−680.
34. Calugaru, S. V., Swanson, R., and Olson, S. T. (2001) *J. Biol. Chem.* (in press).
35. Hess, G. P., McConn, J., Ku, E., and McConkey, G. (1970) *Philos. Trans. R. Soc. London, Ser. B 257*, 89−104.
36. Sigler, P. B., Blow, D. M., Matthews, B. W., and Henderson, R. (1968) *J. Mol. Biol. 35*, 143−164.
37. Huber, R., and Bode, W. (1978) *Acc.Chem. Res. 11*, 114−122.
38. Hedstrom, L., Lin, T.-Y., and Fast, W. (1996) *Biochemistry 35*, 4515−4523.
39. Jencks, W. P. (1987) *Catalysis in Chemistry and Enzymology*, Dover Publications, New York.
40. Mast, A. E., Enghild, J. J., Pizzo, S. V., and Salvesen, G. (1991) *Biochemistry 30*, 1723−1730.

BI015650+